

6D Cooling using Non-Flip lattices
 R. B. Palmer, R. Fernow
 Brookhaven National Laboratory
 10/18/2012

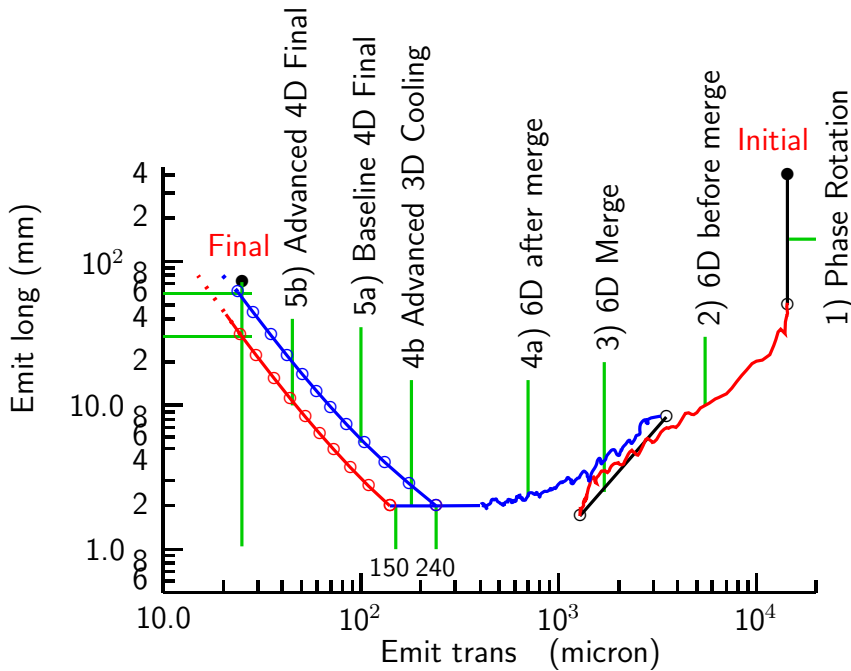


Figure 0: Emittance evolution in a simulation of 6D cooling after the 6D merge, using RFOFO lattices

1 Introduction

The concept[?] for ionization cooling for a muon collider can be represented by an emittance evolution plot (fig. 2) and consists of a sequence of the following subsystems:

1. Phase Rotation[?] that converts the initial single distribution of muons into 12 separate bunches spaced at 201.25 MHz
2. Initial 6D cooling in channels that are curved into gentle upward or downward helices Guggenheims[?].
3. Bunch merging that combines the 12 bunches of each sign into single bunches. This is done by a factor of 3 in longitudinal phase space and by a factor of 2 in each transverse phase space.
4. More 6D cooling taking the normalized rms longitudinal emittances to not less than 2 mm, from space charge considerations, and as low as possible in the transverse directions. We will consider two options here:
 - (a) Cooling to 240 μm in transverse emittances - taken as the baseline solution, and
 - (b) Cooling to 150 μm in transverse emittances - taken as the 'advanced' solution.
5. 'Final Cooling in approximately 12 liquid hydrogen absorbers in 40 T long solenoids, with re-acceleration and matching in lower fields between each high field magnet. Depending on the previous 6D cooling there are two differing final cooling designs:
 - (a) Cooling to the required transverse emittance of 25 μm and longitudinal emittance of about 6 mm
 - (b) Cooling to the required transverse emittance of 25 μm and longitudinal emittance of about 3 mm. The lower longitudinal emittance is much preferred for the acceleration.

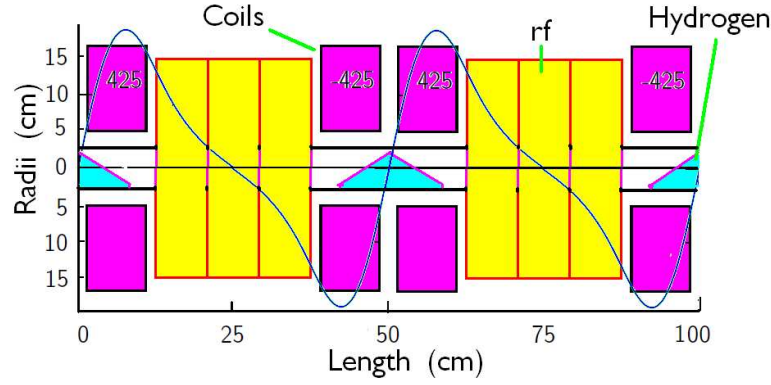


Figure 1: Section through a late stage RFOFO 6D cooling lattice in which the fields reverse both across the absorber and the rf

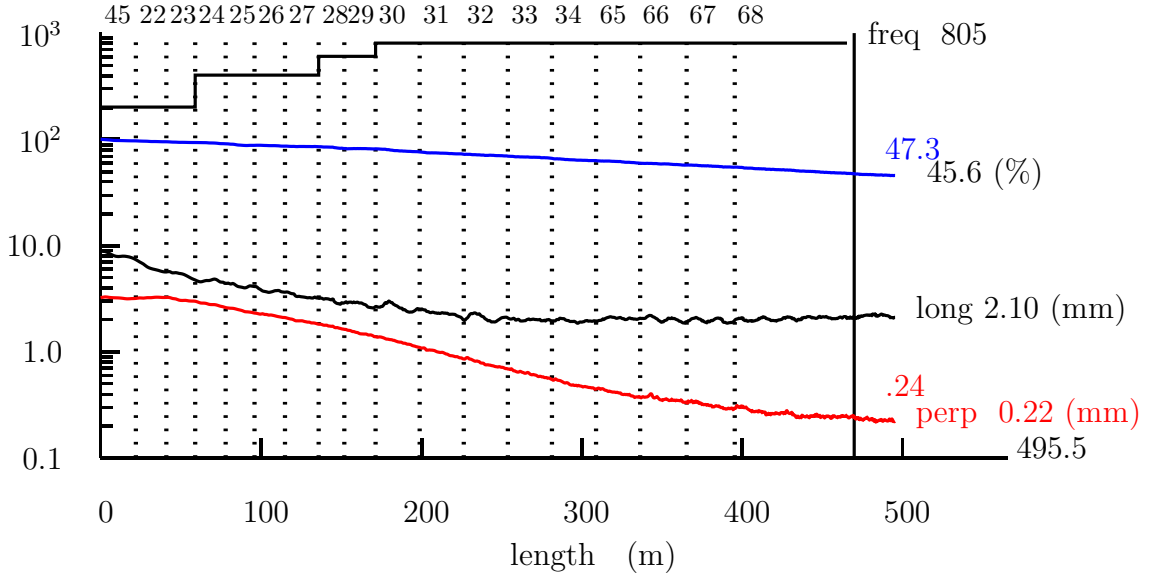


Figure 2: Emittances and transmission vs. length in a 6D cooling system using only RFOFO lattices.

2 Case #1 using only RFOFO (flip) Lattices

A design for 6D cooling using only FOFO or RFOFO lattices has been presented before[?]. It consisted of sequences of "stages". Each stage contains a strings of identical cells. The early stages employ cells of 2.75 m length and use 210.25 MHz rf. For later stages, the cells get shorter and the rf frequency rises to 805 MHz. Fig. 1 shows one, relatively late, cell of such a lattice.

The solenoid coils are tilted (not shown here) by a few degrees to generate a vertical field that bends the lattice and generates dispersion. The absorbers are wedge shaped to generate emittance exchange for longitudinal cooling.

In the initial stage, when the transverse emittance is large, the focusing must be relatively weak to avoid excessive angular distributions. But the weak focusing implies that the equilibrium emittance is also relatively large, so that the transverse cooling weakens as this limit is approached. To avoid this, this stage is terminated and we couple into the next stage that has stronger focusing. This sequence of stages with ever stronger focusing is termed 'tapering'.

An ICOOL simulation used 6000 initial muon tracks taken from the output of a simulation of a 6D merge[?]. For a first estimate of performance of the cooling sequence, the simulation was done of a straight sequence of lattices with simple cylindrical hydrogen absorbers with flat ends and windows.

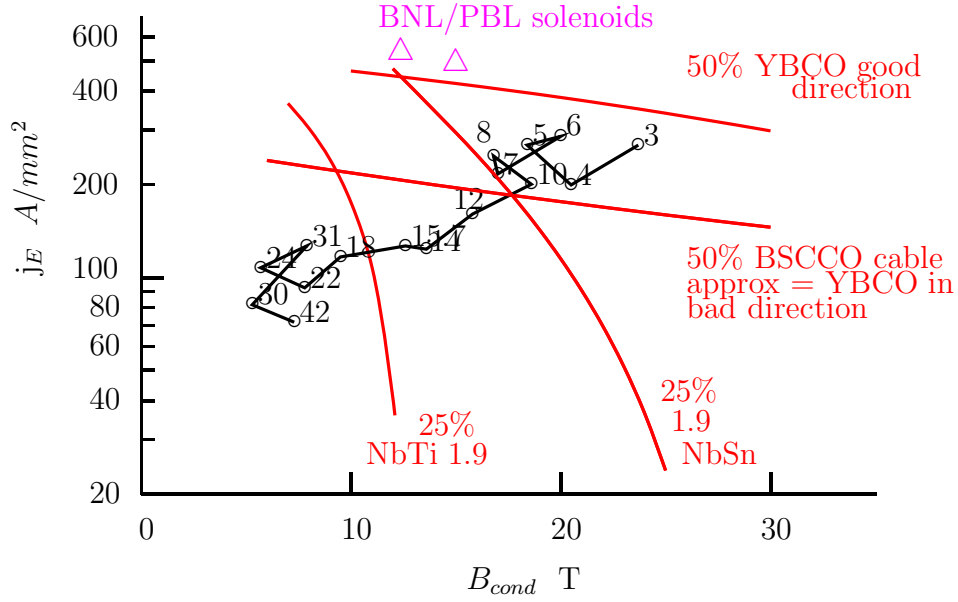


Figure 3: Current densities vs. local magnetic fields: in black for stages using RFOFO (flip) lattices for betas. Numbers after point show absorber β s in cm. Red lines show plausible engineering limits for different conductors.

Since such a simulation has no real emittance exchange, such exchanges were applied by a transport matrix acting on $(x, x', y, y', \sigma_z, \sigma_p/p)$ introduced before each cell. The matrix used was of the form:

$$\begin{pmatrix} 1 & 0 & 0 & 0 & 0 & 0 \\ 0 & 1 + \delta & 0 & 0 & 0 & 0 \\ 0 & 0 & 1 & 0 & 0 & 0 \\ 0 & 0 & 0 & 1 + \delta & 0 & 0 \\ 0 & 0 & 0 & 0 & 1 & 0 \\ 0 & 0 & 0 & 0 & 0 & 1 - 2\delta \end{pmatrix}$$

with the values of δ adjusted to get the required exchange. Transition from one stage to the next was done with artificial 'hard' ends at absorber centers where the axial magnetic fields are always zero. However, the transverse magnetic fields off axis are non-zero and are somewhat different from one stage to the next. So the hard transition is not strictly Maxwellian.

Fig2 shows emittances and transmission as a function of length along the cell axes. The vertical dotted lines define the transitions between stages and the numbers at the top of these dotted lines give the file numbers for the differing lattices. The transverse emittance is seen to fall to the baseline requirement of 240 μm after a distance of 470 m. The longitudinal emittance is there (2.1 mm) approximately 2 mm, as specified, and the transmission is 47.3%, which is probably acceptable.

There are two problems:

- This system does not cool to a low enough transverse emittance to allow the 'advanced' solution.
- The current densities in the super-conductors are too high for the calculated local field maxima.

Fig. 3 Shows the current densities vs. the maximum local fields in the coils used. The red lines represent estimates of what is plausible. For these estimates we have used published[?] 'engineering' current densities, multiplied by factors to allow the required support structure, the need for stabilizing copper, and the filling factor for a real conductor. We estimate this factor to be approximately 25% for NbTi, Nb₃Sn cable, about 50% for BSCCO cable, and 50% for YBCO tape when used for non-flip designs where the fields are approximately aligned with the tape surfaces. Note that two experimental dipoles[?], plotted as triangles in magenta, have achieved fields above this assumed limit.

With these assumptions, the bounds for NiTi and Nb₃Sn at 1.9 deg. are shown on the plot. It appears that for the lattices with betas less than 7 cm, the requires current densities are too high for Nb₃Sn. They are also above the estimate for BSCCO HTS coils.

Unfortunately, for these RFOFO lattices, with their rapidly changing axial fields, the field lines are very far from this 'good' direction, and we find the current needed for the small β s cannot be obtained YBCO.

However, it appears that the needed fields could be achieved if a design is used in which the fields are approximately aligned with the tape surfaces, such as a Fernow (non-flip) lattice.

3 Case #2 With initial RFOFO and later Fernow (Non-flip) lattices

To avoid the build up of angular momentum, it is desirable to have axial fields that alternate. In the simple case of cooling in a uniform field, this effect effectively terminates the cooling after some significant distance. The problem, as we shall see, is not so severe in periodic lattices, but has remained the argument that has favored lattices where the field reverses in the center of every absorber.

To avoid resonances, it is desirable that all cells are identical. This, together with the angular momentum argument, has been the basis for using the 'Reverse-Focus-Focus', or RFOFO lattices as shown in figs. 1 and ?? . But now we see that the rapid field changes intrinsic to an RFOFO lattice but an excessive demand on the needed super-conductors, and we are now considering a lattice[?] proposed by Rick Fernow. A particular advantage of this lattice is that it can use only one coil per cell, and this coil is not naturally located over the rf, thus simplifying the design. An example of such a lattice is shown in fig. 4. In fig. 5, for lattices with betas less than 7 cm, the required current densities for such Fernow lattices are plotted against the maximum fields in the coils. The requirements for the RFOFO lattices with betas less than or equal to 7 cm are also shown.

It is seen that the required current densities are significantly lower for the Fernow lattices, allowing lattices with betas down to 3.4 cm to use Nb₃Sn conductor. For lattices with smaller betas, down now to 1.8 cm, the current densities are too high for Nb₃Sn and for BSCCO. But they are below the estimated limit for YBCO for fields in the 'good' direction. But now the fields are indeed in the 'good' direction, being somewhat better than the directions in a simple stand alone solenoid like those built and tested by a collaboration of Brookhaven National Lab (BNL) and Particle Beam Lasers (PBL)[?]. The densities and fields in those coils are also plotted and form the basis for putting the limit at 60% of the published conductor performance.

Using these RFOFO and Fernow lattices, an ICOOL simulation using matrix emittance exchange, as above, gave emittances and transmissions as shown in fig.6. Parameters of the lattices, rf and absorbers are given in the appendix tables ?? and ??. Cooling to the 'baseline' transverse emittance of 240 μm is now achieved in a somewhat shorter distance of 430 m (470 m), with about the same transmission of 48% (47.3%). But it can still not get the emittance down to the 150 μm required for the 'advanced' specification, despite the much lower design betas of 1.8 mm (3.4 mm).

To understand this result, it is useful to look at the beam betas of the muons being cooled. These are shown in fig. 7, together with the design betas of the lattices used. It is observed that whereas the beam and design betas agree in the RFOFO stages, the beam betas are very significantly higher than the design betas in the Fernow non-flip stages. The explanation is simple: solenoid magnetic focusing comes from the interaction of particles azimuthal momentum interacting with the solenoidal field; where the azimuthal momentum was generated by the entry of the particles into the solenoid. In the absence of absorbers, this azimuthal momentum is given by:

$$p_\phi = \frac{A_c}{r} - \frac{r}{2} \frac{q}{B_z}$$

where A_c is the particles Canonical angular momentum (i.e. its angular momentum before it entered the field), r is the radius of the particle, and B_z is the local axial field. But an absorber cools the transverse momenta INCLUDING the p_ϕ above. This results in a coherent rise in the canonical angular momenta. Fig. 8 shows the average p_ϕ and $(p_\phi)_{\text{canonical}} (= r A_c)$, together with the axial fields on the absorbers, as a function of length down the channel. It is seen that p_ϕ , instead of rising linearly with the axial fields, after an initial rise, falls as it travels down the channel. This explains why there is less focusing, and larger beam betas, than calculated assuming no average canonical angular momentum.

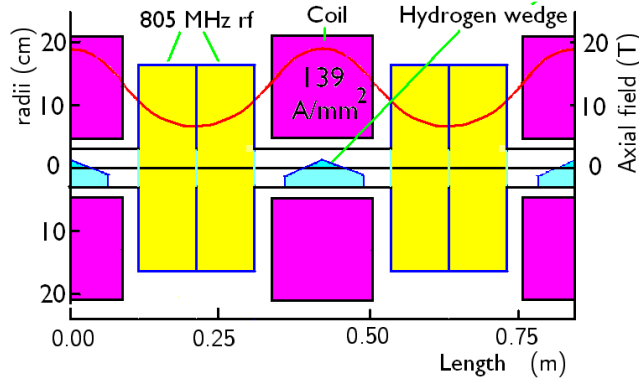


Figure 4: Section through a late stage of a Fernow (non-flip) lattice in which the fields maintain the same polarity

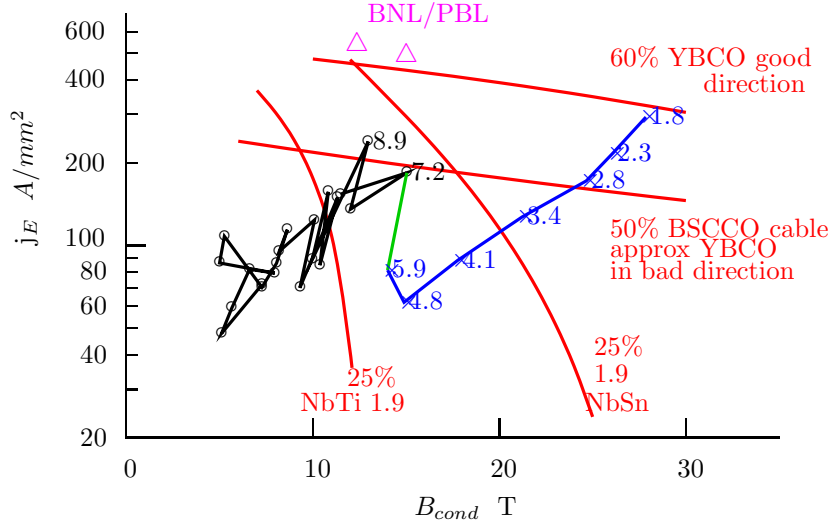


Figure 5: Current densities vs. local magnetic fields: in black for stages using RFOFO (flip) lattices for betas ≤ 7 cm; and in blue for Fernow (non-flip) lattices for those with betas < 7 cm. Numbers after point show absorber β s in cm.

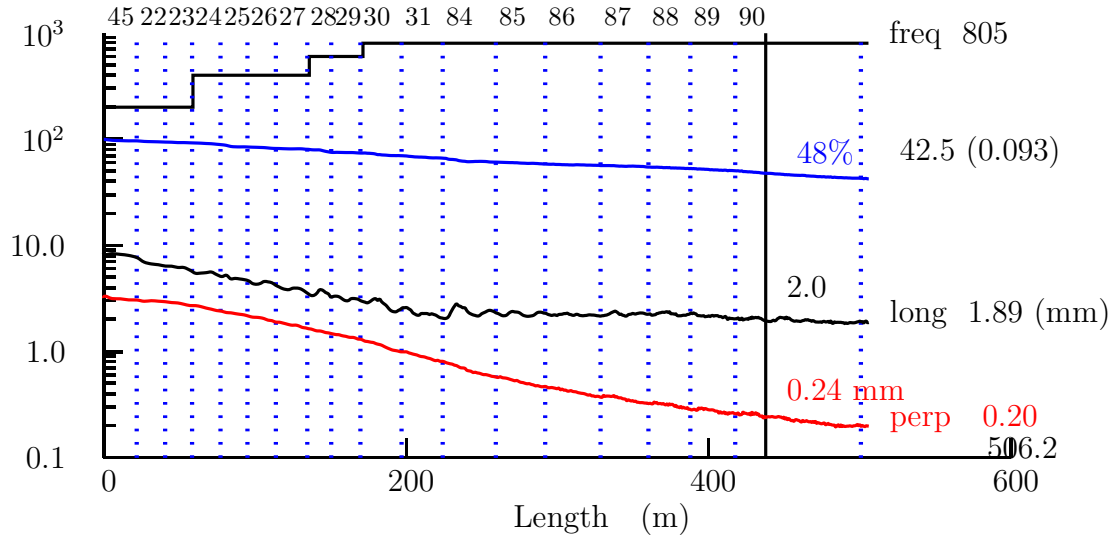


Figure 6: ICOOL simulated emittances and transmission for the 6D cooling channel with initial stages using RFOFO (flip) lattices, followed by later stages using Fernow (non-flip) lattices.

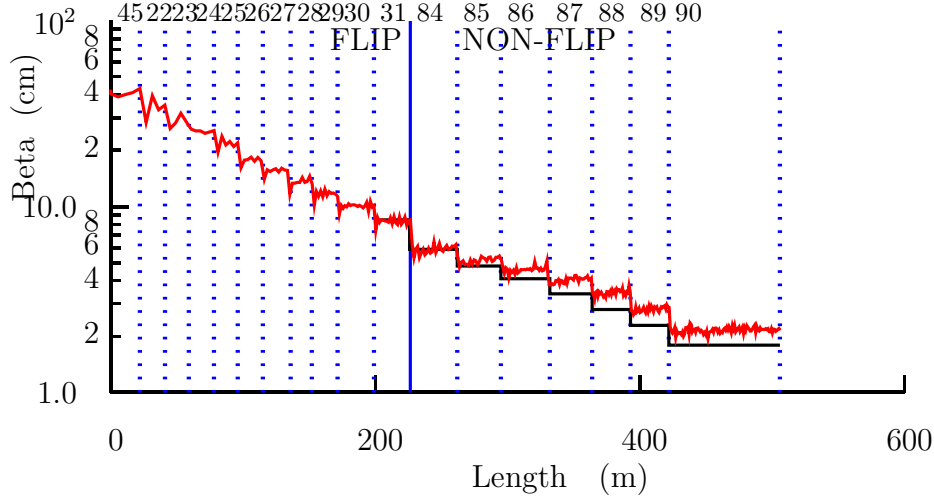


Figure 7: Simulated beta functions β_{\perp} in red, together with those calculated for stand alone lattices (black), for simulated in the combined RFOFO (flip) and Fernow (non-flip) lattices

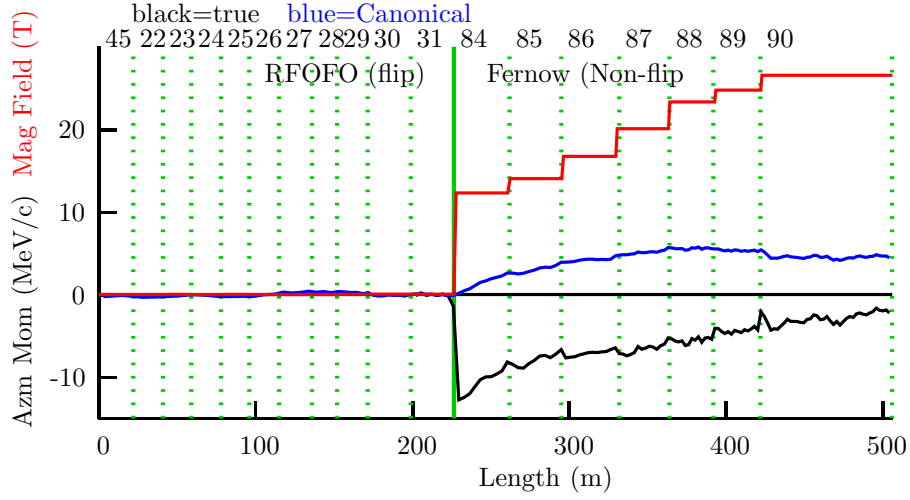


Figure 8: Simulated average azimuthal momenta, and the canonical azimuthal momenta, under the rf, together with the axial magnetic fields at the absorber centers, for simulated in the combined RFOFO (flip) and Fernow (non-flip) lattices

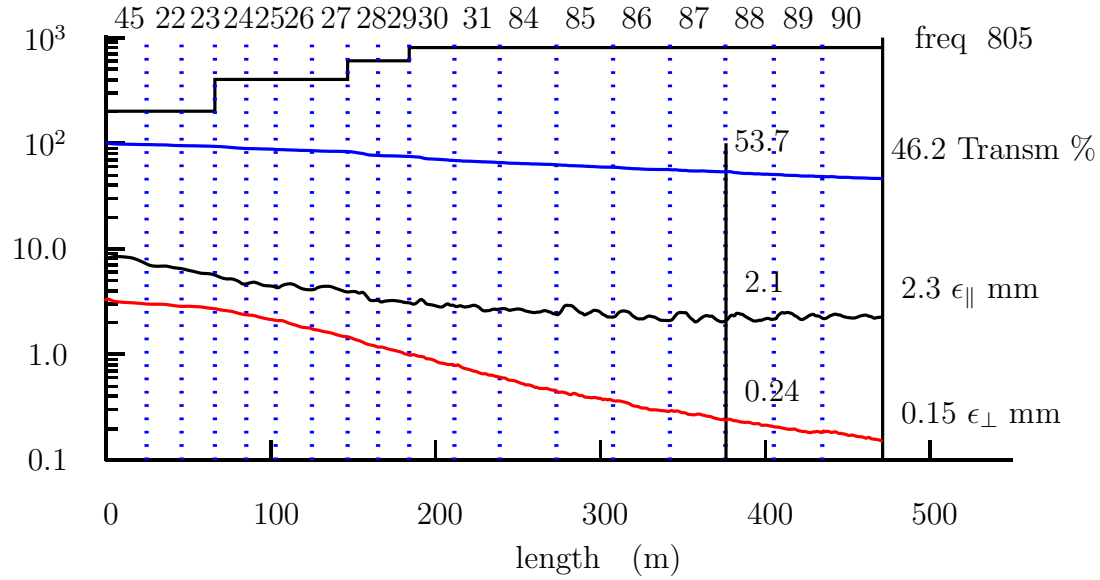


Figure 9: ICOOL simulated emittances and transmission for an improved 6D cooling channel with field reversals introduced between the Fernow (non-flip) stages.

4 Case #2 with initial RFOFO and later Fernow (Non-flip) lattices

Figure 9 and table1 shows the results of an ICOOL simulation in which, 'hard' field reversals have been inserted between the stages of the Fernow (non-flip) stages. Figure ?? shows the field reversals between stages. It also shows the simulated average azimuthal momenta, and average canonical azimuthal momenta. The average azimuthal momenta now alternate, but no longer show a dramatic fall off with length, and the average canonical azimuthal momenta no longer rise monotonically, as before.

The transmission to reach the 'baseline' transverse emittances is now significantly better: 53.7 % compared with 48%. And now we do achieve cooling to the advanced specification of $150 \mu\text{m}$ with a transmission of nearly 46.2%, the same as achieved for the baseline without reversals.

The question is now whether we can design the required field reversals without excessive super-conductor current densities. This can probably be done by first matching, with rf but without absorbers, the high field non-flip to a lower field, and thus higher beta, lattice. Now the field reversal should be relatively easy. This would be followed by a match back into the higher field non- flip lattice. But this has yet to be demonstrated, and will, in any case require some added length and losses.

An attempt was made to use Fernow non-flip lattices also for the earlier stages. So far this resulted in poor transmission (see table 2). The problem appears to be a difficulty in maintaining enough longitudinal acceptance when the momentum spread is still large. One possible explanation is that the occasional field reversals introduce excessive sudden changes in the forward velocities of particles with finite canonical moments. Another is that the smaller, but finite changes in the focusing strength with the finite average canonical azimuthal momenta, cause the resonances that limit the angular acceptance to shift. This later effect could be corrected by appropriate shifts in the focus currents within a stage. The only cure for the former effect would be to increase the frequencies of the reversals. At this point it seems wiser to keep the RFOFO lattices where their conductor requirements can be met, and use the Fernow lattices only when this is no longer the case.

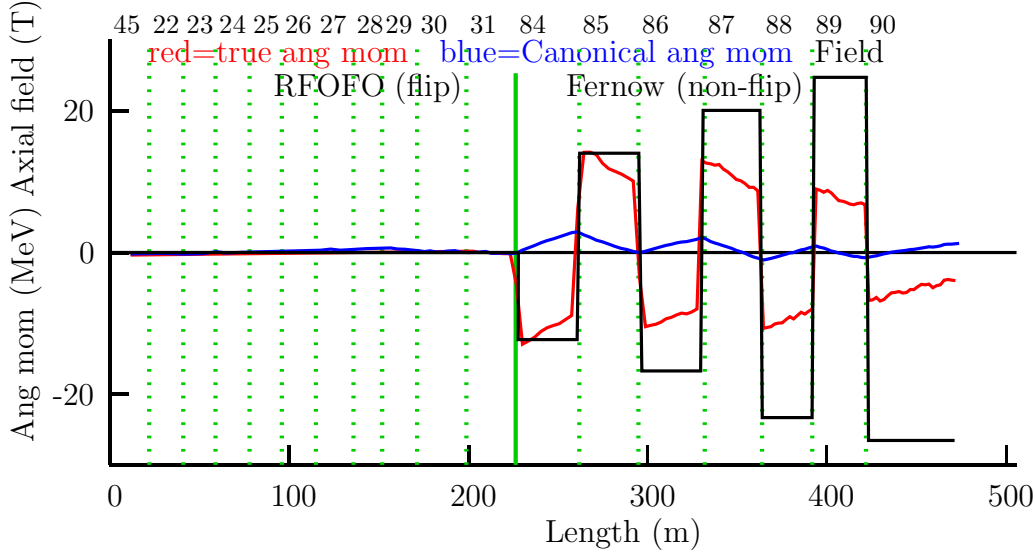


Figure 10: Simulated average azimuthal momenta (black), and average canonical azimuthal momenta (blue), between the absorbers, vs. length, together with the magnetic fields (red) at the absorber centers (red), in the improved combined RFOFO (flip) and Fernow (non-flip) lattices

5 Parameters and discussion of case #3

The dimensions and current densities of coils in the lattices are given in table 4. Table 3 defines the dimensions shown in this table: a) for the RFOFO cases indicated with "f" in the third column, and b) the Fernow (non-flip) stages indicated by "nf".

All cells are either left right symmetric or anti-symmetric. The length dimensions refer to the distances from the ends of the cells. In the cases with $L1$, $dL2$, $R2$, $dR2$, & $J2=0$, then there are just two coils per cell; in the RFOFO case these have opposite polarities. In the Fernow cases, they have the same polarities.

When there are dimensions given for $L1$ etc and $L2$ etc, then there are four coils per cell: two in the first half and another symmetric, or antisymmetric, pair in the second half.

In many of the Fernow cases, the z position of the start of the coils ($L1$) is zero. In these cases the coil dimensions given define just half the coil: the second half of the full coil of length $2 \times dL1$, and there are then only a single full coil per cell.

Table 5 gives some parameters that follow from the coil parameters in table 4. The value of β is that at the planes defining the cell ends, and this is at the center of the absorbers. It is calculated for a momentum of 200 MeV/c for particles with zero canonical angular momentum, i.e particles that would have no angular momentum if they axially exited from the fields. In the case of the RFOFO lattices, this is just the angular momentum at the cell ends, since the axial field at those locations is zero. In the Fernow non-flip lattices, however, it is non zero.

B_0 in table 5 is the maximum value of the axial field on axis. Bc_1 and Bc_2 are the maximum fields in conductors in the first and second coils. T_1 and T_2 are the maximum hoop stresses in the conductors, where $T = B_z R j$, R is the radius, and j is the current density.

B_{rf} is the maximum axial field where there is an rf cavity whose dimensions are given below. At the end, these fields are of the order of 12 T. Whether such fields will cause damage to the assumed Be walls of the cavity is not yet known and cannot be experimentally determined with rf tests in the 3.5-4 T 'Lab G' magnet. Determining this limit will be important.

Table 6 gives parameters for, parameter δ (see section *** above) that determines the emittance exchange, the liquid hydrogen absorbers, the aluminum absorber windows, and the rf cavities. A single absorber window is simulated, but its thickness is assumed to cover both actual window and a second safety window. The windows are simulated as flat, and of constant thickness, although they would in reality be shaped.

The rf cavities are simulated as perfect pill-boxes with flat windows. There are n_{rf} cavities, each of

Table 1: Emittances and transmission for case #3

i	file	typ	leng m	ϵ_{\perp} mm	ϵ_{\parallel} mm	Transm %
1	45	f	25	2.991	6.96	97.0
2	22	f	46	2.854	6.50	95.0
3	23	f	66	2.710	5.65	93.3
4	24	f	85	2.362	4.73	88.9
5	25	f	103	2.091	4.29	87.1
6	26	f	125	1.723	4.13	84.9
7	27	f	147	1.471	3.90	83.3
8	28	f	165	1.174	3.24	76.6
9	29	f	184	0.983	3.06	74.9
10	30	f	211	0.784	2.85	68.4
11	31	f	239	0.606	2.70	65.7
12	84	nf	273	0.444	2.38	62.5
13	85	nf	308	0.364	2.27	59.2
14	86	nf	342	0.294	2.12	56.0
15	87	nf	376	0.240	2.10	53.7
16	88	nf	405	0.207	2.16	50.6
17	89	nf	435	0.188	2.18	48.4
18	90	nf	471	0.150	2.26	46.2

length L_{rf} in each cell. They are symmetrically located. The needed radii of these windows are given as R_{rf} , but their effects were not included in these simulations.

Table 7 gives a few derived quantities.

δ/L_{abs} is a metric proportional to the simulated fractional longitudinal cooling that comes from emittance exchange acting on the transverse cooling proportional to the absorber length. We assume that the cost of the enormous 201 MHz cavities, and rf power, will be a significant cost driver. Thus the emittance exchange is high at the start in order to bring down the longitudinal emittance and allow early switching to higher frequency rf. Consideration of longitudinal space charge effects[?] suggest that the longitudinal emittance should not be reduced below approximately 2 mm. Thus, after this goal has been reached, the emittance exchange is only large enough to stop the longitudinal emittance from rising.

$n_{rf}L_{rf}/L_{cell}$ gives the total fraction of cell length full of rf. It is initially quite large (67.8%) but has to be reduced later as the absorber lengths are reduced, and to accommodate the increasingly demanding coil requirements. This fraction ignores the real need for some spaces between cavities.

L_{abs}/L_{cell} , initially, is chosen to give energy loss equal to the gain from the rf with the chosen gradient of 16.5 MeV/m and the chosen phase advance of 34 degrees. Later the absorber fraction is reduced to keep L_{abs}/β (the absorber length divided by the calculated β) below 1.0, to avoid excessive enhanced scattering at the ends of each absorber.

β/β_o is the ratio of calculated β to the β that would be obtained with a continuous solenoid of field equal to the maximum (B_o) in the lattice used. Initially this is close to one, and the only reason not to use the continuous solenoid is the need, early on, to frequent field reversals. Later, the ratio falls as we use the periodic lattices to generate locally lower β s at the periodic foci where the absorbers are located.

6 Summary and Conclusion

The simulated performance of four cases are summarized in table ??.

Table 2: Summary of simulations

case	files		$\epsilon_{\perp}=240 \mu\text{m}$			$\epsilon_{\perp}=150 \mu\text{m}$		
			Length	ϵ_{\parallel}	Transm. %	Length	ϵ_{\parallel}	Transm. %
1	tap16a0	RFOFO lattice with flips	470	2.1	47.3			
2	tap16a4	Non-flip lattices for $\beta < 7$ cm	430	2	42.5			
3	tap16a5v	" with flips between stages	375	2.1	53.7	471	2.15	46.2
4	tap16a14	" starting Non-Flips earlier	377	2.56	45.9	473	2.38	38.5

This is the favored case with Fernow non flip lattices only used for the later stages where the current density requirements for the solenoids are excessive. Figure ?? define the dimensions used in table ??.

CONCLUSION NEEDED HERE

SECTIONS OF LATTICES AND BETAS VS MOMENTUM ALSO NEEDED

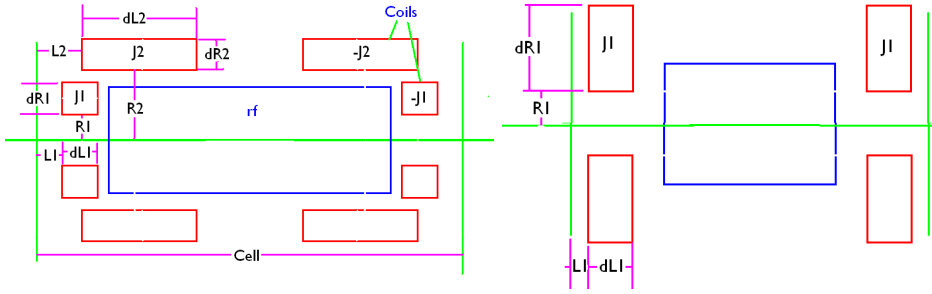


Table 3: Definitions of terms in table ??: a) for RFOFO (flip cases), b) for Fernow (non-flip) cases

Table 4: Coil parameters of case #3

file	typ	cell cm	L_1 cm	dL_1 cm	R_1 cm	dR_1 cm	j_1 A/mm ²	L_2 cm	dL_2 cm	R_2 cm	dR_2 cm	j_2 A/mm ²
1	45	f	275.0	30.5	80.5	77.0	92.0	72.3	0.0	0.0	0.0	0.0
2	22	f	235.7	13.7	29.1	42.9	55.7	48.0	25.7	94.3	70.3	83.1
3	23	f	202.1	12.5	24.3	36.7	47.8	82.1	22.0	80.8	69.8	84.5
4	24	f	173.2	9.5	22.0	25.2	31.5	86.6	18.9	69.3	37.8	44.1
5	25	f	148.5	8.1	18.9	24.3	38.9	70.6	16.2	59.4	41.6	55.1
6	26	f	137.5	6.5	18.5	22.5	32.5	114.4	15.0	55.0	38.5	51.0
7	27	f	127.3	6.9	16.2	18.5	32.9	124.1	11.6	53.2	39.3	62.5
8	28	f	115.4	6.3	14.7	16.8	29.8	149.8	10.5	48.3	35.7	56.6
9	29	f	99.5	5.4	12.7	10.9	22.1	157.1	9.0	41.6	25.3	43.4
10	30	f	80.6	4.4	10.3	8.8	17.9	239.4	7.3	33.7	20.5	35.2
11	31	f	68.8	3.8	13.8	7.5	15.3	184.3	6.3	28.8	17.5	30.0
12	84	nf	68.8	3.4	13.8	8.4	37.7	81.6	0.0	0.0	0.0	0.0
13	85	nf	68.8	0.0	13.8	7.1	36.4	-62.3	0.0	0.0	0.0	0.0
14	86	nf	57.5	0.0	11.5	5.9	30.6	88.5	0.0	0.0	0.0	0.0
15	87	nf	48.0	0.0	9.6	5.0	25.5	-127.3	0.0	0.0	0.0	0.0
16	88	nf	42.0	0.0	8.4	4.2	21.6	172.1	0.0	0.0	0.0	0.0
17	89	nf	42.0	0.0	8.4	4.2	18.0	-217.0	0.0	0.0	0.0	0.0
18	90	nf	42.0	0.0	8.4	4.2	14.4	293.7	0.0	0.0	0.0	0.0

Table 5: Fields and Coil Hoop Stress for case #3

file	typ	beta cm	B_0 T	B_{rf} T	B_{c1} T	B_{c2} T	T_1 MPa	T_2 MPa
1	45	f	42.5	2.74	2.74	7.27	0.00	409
2	22	f	37	3.10	3.10	5.10	5.66	95
3	23	f	30.6	3.63	3.63	6.61	7.96	196
4	24	f	26.6	4.18	4.18	5.00	5.26	111
5	25	f	22	4.91	4.91	7.27	8.05	126
6	26	f	18.1	5.43	5.43	8.63	8.20	221
7	27	f	15	6.01	6.01	10.09	9.30	241
8	28	f	13.8	6.58	6.58	11.32	10.38	297
9	29	f	11	7.66	7.66	10.83	9.97	210
10	30	f	8.9	9.46	9.18	12.97	12.02	300
11	31	f	7.2	11.66	10.01	15.04	11.49	261
12	84	nf	5.9	12.32	8.84	14.01	0.00	156
13	85	nf	4.8	14.03	8.62	14.89	0.00	111
14	86	nf	4.1	16.73	10.30	17.76	0.00	159
15	87	nf	3.4	20.08	12.37	21.22	0.00	225
16	88	nf	2.8	23.32	12.06	24.66	0.00	299
17	89	nf	2.3	24.75	11.85	26.08	0.00	350
18	90	nf	1.8	26.55	11.57	27.86	0.00	435

Table 6: c)Absorber and rf parameters for case #3

i	file	typ	leng m	n	cell cm	delta	Labs cm	Rabs cm	Lwin μ m	nrf	Lrf cm	f MHz	grad MV/m	ph deg	Rrf cm
1	45	f	25	9	275.0	0.0260	21.31	15.0	500	5	37.29	201	16.5	34.0	21.5
2	22	f	46	9	235.7	0.0220	18.27	13.2	430	4	39.95	201	16.5	34.0	18.7
3	23	f	66	10	202.1	0.0190	15.66	12.0	367	4	34.26	201	16.5	34.0	16.2
4	24	f	85	11	173.2	0.0150	13.42	11.0	315	6	19.57	402	16.5	34.0	14.1
5	25	f	103	12	148.5	0.0130	11.51	10.0	280	5	20.14	402	16.5	34.0	11.8
6	26	f	125	16	137.5	0.0110	10.66	8.0	231	5	18.64	402	16.5	34.0	10.2
7	27	f	147	17	127.3	0.0090	9.87	7.0	198	6	14.38	402	16.5	34.0	9.1
8	28	f	165	16	115.4	0.0070	8.94	6.1	170	5	15.65	603	16.5	34.0	7.3
9	29	f	184	19	99.5	0.0060	7.71	5.4	146	5	13.49	603	16.5	34.0	7.0
10	30	f	211	34	80.6	0.0055	7.61	4.4	125	5	9.67	805	22.7	34.0	6.0
11	31	f	239	40	68.8	0.0050	5.41	3.8	104	4	8.59	805	22.7	34.0	5.5
12	84	nf	273	50	68.8	0.0040	5.41	2.8	100	4	8.59	805	22.7	34.0	5.2
13	85	nf	308	50	68.8	0.0035	4.80	2.2	100	4	8.59	805	22.7	29.8	4.8
14	86	nf	342	60	57.5	0.0030	4.10	1.8	100	3	9.58	805	22.7	30.2	3.9
15	87	nf	376	70	48.0	0.0025	3.40	1.6	100	3	8.00	805	22.7	30.0	3.3
16	88	nf	405	70	42.0	0.0022	2.78	1.3	100	2	8.83	805	22.7	34.0	2.8
17	89	nf	435	70	42.0	0.0017	2.30	1.2	100	2	9.13	805	22.7	26.5	2.7
18	90	nf	471	86	42.0	0.0010	1.80	1.1	100	2	9.45	805	22.7	19.8	2.7

Table 7: Some general parameters for case #3

i	file	typ	δ/L_{abs} cm^{-1}	$n_{rf}L_{rf}/L_{cell}$ %	L_{abs}/L_{cell} %	L_{abs}/β %	β/β_B
1	45	f	0.122	67.8	7.75	50.1	0.87
2	22	f	0.120	67.8	7.75	49.4	0.86
3	23	f	0.121	67.8	7.75	51.2	0.83
4	24	f	0.112	67.8	7.75	50.5	0.83
5	25	f	0.113	67.8	7.75	52.3	0.81
6	26	f	0.103	67.8	7.75	58.9	0.74
7	27	f	0.091	67.8	7.75	65.8	0.68
8	28	f	0.078	67.8	7.75	64.8	0.68
9	29	f	0.078	67.8	7.75	70.1	0.63
10	30	f	0.072	60.0	9.44	85.4	0.63
11	31	f	0.092	50.0	7.86	75.1	0.63
12	84	nf	0.074	50.0	7.86	91.6	0.55
13	85	nf	0.073	50.0	6.98	100.0	0.51
14	86	nf	0.073	50.0	7.13	100.0	0.51
15	87	nf	0.074	50.0	7.08	100.0	0.51
16	88	nf	0.079	42.1	6.62	99.2	0.49
17	89	nf	0.074	43.5	5.48	100.0	0.43
18	90	nf	0.056	45.0	4.29	100.0	0.36